[1,*]Fenghe Jin
[2]Xin Yu
[3]Zhenyu Song

LCL-T Module Reduction of Offshore Photovoltaic Power Generation System Based on Current Feedback-routh Approximation Method

Journal of Electrical Systems

Abstract: - The rapid development of offshore photovoltaic power generation has attracted more and more attention. Aiming at the problem of poor output power quality caused by the randomness and intermittentness of offshore photovoltaic power generation, LCL filters and isolation transformers are widely used on the AC side of photovoltaic power generation systems to improve the power quality of Grid-connected. Although this method has a good suppression effect on harmonics and DC components, its higher order will result in a larger amount of calculation, especially in the simulation of large-scale photovoltaic grid-connected systems, the operating speed will be too slow. In order to increase the simulation rate while ensuring the quality of the output power, the high order LCL-T (LCL filter and isolation transformer) module of the photovoltaic power generation system is reduced in order. When the transformer is not saturated, the LCL-T module reduction method based on the weighted current feedback method is adopted, and the purpose of simplification is achieved through the zero-pole cancellation of the transfer function; When the transformer is saturated, the LCL-T module reduction method based on the Routh approximation method is adopted, Use advanced mathematics formulas to reduce the order of high-order system equivalent processing. The PSCAD/EMTDC simulation software verifies the off-grid characteristics and simulation rate of the reduced-order model.

Keywords: Offshore Photovoltaic Power Generation System, Reduced Order Model, Lcl-T, Current Feedback Method, Routh Approximation Method.

I. INTRODUCTION

In recent years, offshore photovoltaic power generation has gradually emerged. The installed capacity of near-shore and offshore photovoltaic power generation systems has developed rapidly and has been extensively studied by scholars at home and abroad [1-3]. Large-scale photovoltaic power generation systems continue to penetrate into the grid, making the network structure intricate and inconvenient to study the impact of its grid connection [4].

The higher model order of the photovoltaic power generation system leads to a larger amount of calculation, which brings problems such as model validity, data modification, large memory usage and long simulation time [5-10]. At present, the simplification is mainly focused on the inverter topology and its control strategy.S ome literature aims at the topology of the LC-T grid-connected inverter, using weighted current feedback method to achieve model reduction, the reduced-order model has good dynamic and static response capabilities and harmonic suppression capabilities [11].

Some research use the split capacitor method to simplify the processing of the grid-connected inverter, and reduce the third-order system to the first-order system through the zero-pole cancellation method, and the control object is equivalent to the L-type filter, Reducing the difficulty of inverter control strategy design[12-13]. A paper uses the Thevenin-norton equivalent method to reduce the order of the AC side and inverter link of the LCL photovoltaic power generation system, and simplifies the LCL filter and inverter into an equivalent current source and equivalent conductance series model [14]. The complexity of the system is greatly simplified, but the accuracy is not high. The AC side of the photovoltaic power generation system is the key to the inverter control design, but the current domestic and foreign research on its reduction is not thorough enough.

Power system simulation software PSCAD/EMTDC, PowerFactory/DIgSILENT and Matlab/Simulink have customized module functions and can flexibly build simulation models of photovoltaic power generation system [15-20]. Among them, PSCAD/EMTDC simulation software has absolute advantages in dynamic process of photovoltaic power generation system.

Based on the AC side of the photovoltaic power generation system, this paper studies the reduction method of the LCL-T module of the photovoltaic power generation system, and proposes a reduction model of the LCL-T module of the photovoltaic power generation system based on the current feedback-rouse approximation method.

[1] School of Economics and Management, Northeast Electric Power University, Jilin, Jilin, China
[2] State Grid Jiangsu Electric Power Co., LTD. Yancheng Xiangshui County Power Supply Branch, Yancheng, Jiangsu, China
[3] State Grid Zhejiang Electric Power Co., LTD. Yuyao City Power Supply Company, Ningbo, Zhejiang, China
*Corresponding author: Fenghe Jin

This model considers both the transformer non-saturation and saturation two conditions. When the transformer is not saturated, the LCL-T module reduction method based on the weighted current feedback method is adopted,

The purpose of simplification is achieved through the zero-pole cancellation of the transfer function. When the transformer is saturated, the LCL-T module reduction method based on the Routh approximation method is adopted, and the higher-order system is reduced and equivalently processed by the advanced mathematical formula.

Use the Bode diagram to analyze the feasibility and robustness of the reduced-order model, and use the PSCAD/EMTDC simulation software to verify the External characteristics of the grid-connected characteristics and simulation rate of the reduced-order model of the grid-connected system of 5 photovoltaic power plants with a capacity of 20MW.

II. Mathematical Model of LCL-T Module of Photovoltaic Power Generation System

Figure 1 is a structural diagram of a photovoltaic power generation system. The photovoltaic power generation system includes the DC side (photovoltaic array, DC boost chopper and MPPT control), intermediate links (inverter and its controller), and AC side (filter and transformer).

LCL type filter and isolation. It is one of the main reasons that the simulation running speed is too slow to form a high-order AC system from the transformer. In the figure 1, L_1 and L_2 are the filter inductances, and C is the filter capacitor; the transformer ratio is N_1: N_2; the system frequency is 50Hz.

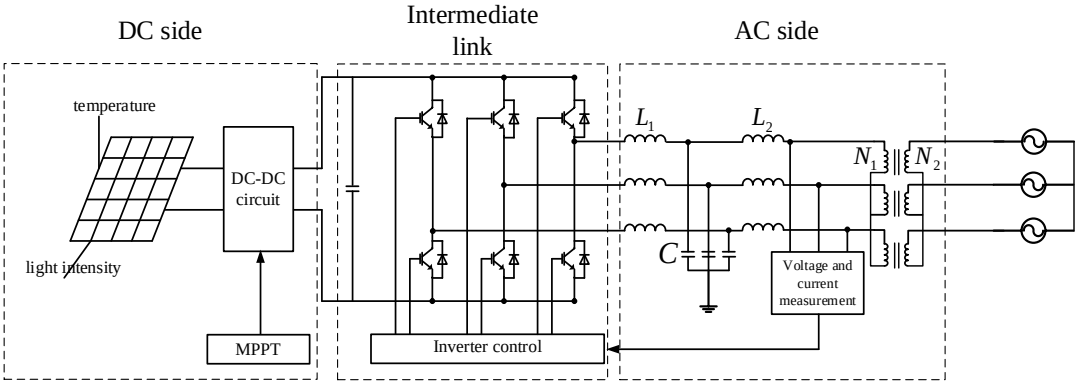

Figure 1: Structure Diagram of Photovoltaic Power Generation System

A. Mathematical Model of LCL-T Module When Transformer is not Saturated

Figure 2 is an equivalent circuit diagram of the AC side when the transformer is not saturated. Take the AC side single-phase structure as an example. Figure 2(a) is the T-type equivalent circuit model of the transformer. L3 and L4 are the primary and secondary inductances after the isolation transformer is equivalent, and Lm is the magnetizing inductance of the isolation transformer. ips and ups are the current and voltage converted to the primary side of the transformer, the single-phase input voltage of the filter is ui, and the output current of the filter L1 is iL. The equivalent circuit of the AC side of the photovoltaic power generation system is a triangular ring circuit composed of the primary, secondary and excitation inductance of the isolation transformer and the filter branch. Figure 2 (b) Using the △/Y transformation theory of the impedance network, the equivalent star impedance network of the isolation transformer is obtained when the isolation transformer is not saturated. The impedances Z1, Z2, and Z3 are shown in equations (1) to (3) respectively.

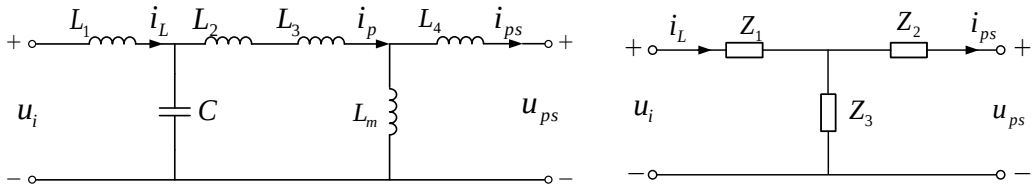

(a) T-type equivalent circuit model of the transformer. (b) The equivalent star impedance network.

Figure 2: Equivalent Circuit Diagram of Ac Side When Transformer is not Saturated

$$Z_1 = sL_1 + \frac{sL_2 + sL_3}{s^2(L_2C + L_3C + L_mC) + 1} \tag{1}$$

$$Z_2 = sL_4 + \frac{s^3(L_2+L_3)L_mC}{s^2(L_2C+L_3C+L_mC)+1} \tag{2}$$

$$Z_3 = \frac{sL_m}{s^2(L_2C+L_3C+L_mC)+1} \tag{3}$$

Applying the principle of superposition, the transfer function between the filter input voltage ui and the transformer primary current ips is shown in equation (4):

$$G_{u_i \to i_{ps}} = \frac{1}{Z_1 + Z_2 // Z_3} \frac{Z_3}{Z_2+Z_3} = \frac{Z_3}{Z_1Z_2 + Z_1Z_3 + Z_2Z_3} \tag{4}$$

In order to meet the requirements of the current feedback method, the transfer function between the filter input voltage ui and the filter L1 output current iL is calculated as shown in equation (5):

$$G_{u_i \to i_L} = \frac{1}{Z_1 + Z_2 // Z_3} = \frac{Z_2+Z_3}{Z_1Z_2 + Z_1Z_3 + Z_2Z_3} \tag{5}$$

B. Mathematical Model of Lcl-T Module When the Transformer is Saturated

Figure 3 shows the equivalent circuit diagram of the AC side when the transformer is saturated. In Figure 3 (a), the same LCL-T module single-phase structure is taken as an example. The transformer adopts a T-type equivalent circuit model. In order to meet the requirements of the reduction method, when the isolation transformer is saturated, the primary, secondary resistances r1, r2 and excitation resistance rm of the transformer are considered. i_{ps}' and u_{ps}' are the current and voltage converted to the primary side of the transformer respectively, and the single-phase input voltage of the filter is u_i', The equivalent circuit of the LCL-T module of the photovoltaic power generation system is a triangular ring circuit composed of the primary, secondary and excitation inductance of the isolation transformer and the filter branch. Figure 3(b) using the △/Y transformation theory of the impedance network, the equivalent star impedance network when the isolation transformer is saturated is obtained. The impedances Z1′, Z2′ and Z3′ are as shown in equations (6)-(8) respectively.

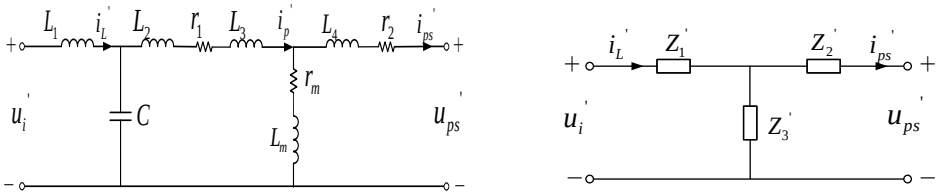

(a) T-type equivalent circuit model of the transformer. (b) The equivalent star impedance network.

Figure 3: Equivalent Circuit Diagram of Ac Side When Transformer is Saturated

$$Z_1' = \frac{r_1+ms}{[s(m+L_m)+r_1+r_m]Cs+1} + L_1s \tag{6}$$

$$Z_2' = \frac{r_m+L_ms}{[s(m+L_m)+r_1+r_m]Cs+1} \tag{7}$$

$$Z_3' = \frac{(r_m+L_ms)(r_1+ms)Cs}{[s(m+L_m)+r_1+r_m]Cs+1} + r_2 + L_4s \tag{8}$$

In the formula: $m=L_2+L_3$.

Calculate the transfer function between the filter input voltage ui′ and the transformer primary output current ips′, and the final simplification is shown in equation (9):

$$G_{u_i' \to i_{ps}'} = \frac{a_1s^5 + a_2s^4 + a_3s^3 + a_4s^2 + a_5s + r_2}{b_1s^6 + b_2s^5 + b_3s^4 + b_4s^3 + b_5s^2 + b_6s + r_mr_2} \tag{9}$$

In the formula:

$a_1=mL_m(m+L_m)C^2+L_4(m+L_m)^2C^2$;

$a_2=[(r_1L_m+mr_m)(m+L_m)+mL_m(r_1+r_m)]C^2+2L_4(m+L_m)(r_1+r_m)C^2+r_2(m+L_m)^2C^2$;

$a_3=r_mr_1(m+L_m)C^2+(r_1L_m+mr_m)(r_1+r_m)C^2+mL_mC+L_4(r_1+r_m)^2C^2+2r_2(m+L_m)(r_1+r_m)$;

$a_4=r_m r_1(r_1+r_m)C^2+(r_1L_m+mr_m)C+r_2(r_1+r_m)^2C^2+2L_4(r_1+r_m)C$;

$a_5=r_m r_1 C+L_4+2r_2(r_1+r_m)C$;

$b_1=L_1L_4(m+L_m)^2C^2+mL_1L_m(m+L_m)C^2$;

$b_2=2L_1L_4(m+L_m)(r_1+r_m)C^2+r_1r_2(m+L_m)^2C^2+L_1(m+L_m)(mr_m+r_1L_m)+mL_1L_m(r_1+r_m)C^2$;

$b_3=2L_1L_4(m+L_m)C+L_1L_4(r_1+r_m)^2C^2+2L_1r_2(m+L_m)(r_1+r_m)C^2+L_1r_mr_1(m+L_m)C^2+L_1(r_1+r_m)(mr_m+r_1L_m)+mL_1L_mC+m^2L_mC+mL_m^2C+L_1L_m(m+L_m)C$;

$b_4=2L_1L_4(r_1+r_m)C+2L_1r_2(m+L_m)C+L_1r_2(r_1+r_m)^2C^2+(2mr_1L_m+m^2r_m)C+L_1r_mr_1(r_1+r_m)C^2+L_1(mr_m+r_1L_m)C+2mL_mr_mC+mr_m^2C+r_1L_m^2C+r_mL_1(m+L_m)C+L_1L_m(r_1+r_m)C$;

$b_5=L_1L_4+2L_1r_2(r_1+r_m)C+L_mr_1^2+2mr_1r_mC+L_1r_mr_1C+L_mL_4+2r_mL_mr_1C+r_mL_1(r_1+r_m)C+L_1L_m+mL_m$;

$b_6=r_1r_2+r_mr_1^2C+L_1r_m+mr_m+r_1L_m+r_m^2r_1C+r_mr_2+r_mL_4$.

III. LCL-T Module Reduction of Photovoltaic Power Generation System Based on Current Feedback-routh Approximation Method

Considering the two situations of transformer non-saturation and saturation, when the transformer is not saturated, the LCL-T module reduction method based on the weighted current feedback method is adopted, and the purpose of simplification is achieved through the zero-pole cancellation of the transfer function; when the transformer is saturated, The LCL-T module reduction method based on the Routh approximation method is adopted, and the higher-order system is reduced and equivalently processed by the advanced mathematical formula.

A. Lcl-T Module Reduction Based on Weighted Current Feedback Method

Based on the dual closed-loop inverter control strategy of voltage outer loop and current inner loop, the current inner loop takes the inverter output current and grid-connected point current as feedback to realize the protection of inverter power switching devices and grid-connected output Power control. The weighted feedback current method is to weight the inverter output current and the grid-connected point current as the feedback value of the current inner loop control, set a proper weighted feedback coefficient, and realize the zero-pole cancellation of the transfer function to achieve the purpose of simplification. Introduce the weighted feedback current i as shown in equation (10):

$$i=\gamma i_{ps}+(1-\gamma)i_L \tag{10}$$

In the formula: γ is the weighted feedback coefficient.

Combining equations (4) and (5), the transfer function between the filter input voltage ui and the weighted feedback current i in the impedance network can be obtained as shown in equation (11):

$$G_{u_i\to i}=\frac{(1-\gamma)Z_2+Z_3}{Z_1Z_2+Z_1Z_3+Z_2Z_3} \tag{11}$$

By substituting Equations (1) ~ (3) into Equation (11), Equation (12) can be obtained by simplification.

$$G_{u_i\to i}=\frac{\{(1-\gamma)(L_2L_4+L_3L_4+L_4L_m+L_2L_m+L_3L_m)s^3C+[(1-\gamma)L_4+L_m]s\}[s^2(L_2+L_3+L_m)C+1]}{[s^2(L_2C+L_3C+L_mC)+1]s^2(a+b)} \tag{12}$$

In the formula:

$a=(L_2L_m+L_3L_m+L_2L_4+L_3L_4+L_4L_m)L_1Cs^2$

$b=L_4L_m+L_1L_m+L_2L_m+L_3L_m+L_1L_2+L_1L_3+L_2L_4+L_3L_4$

Here, if take

$$\gamma=\frac{L_4L_m+L_2L_m+L_3L_m+L_2L_4+L_3L_4}{L_4L_m+L_1L_m+L_2L_m+L_3L_m+L_2L_4+L_3L_4} \tag{13}$$

Then formula (12) can be simplified to formula (14):

$$G_{u_i\to i}=\frac{L_m+(1-\gamma)L_4}{sb} \tag{14}$$

When the transformer is not saturated, the magnetizing inductance L_m is much larger than the primary leakage inductance L_3, the secondary leakage inductance L_4, and the filter inductances L_1, L_2. Therefore, it can be simplified to equation (15):

$$\gamma=\frac{L_4+L_2+L_3}{L_4+L_1+L_2+L_3} \tag{15}$$

Therefore, equation (14) can be further reduced to equation (16):

$$G_{u_i \to i} = \frac{1}{(L_1 + L_2 + L_3 + L_4)s} \tag{16}$$

From equation (16), the model can be reduced to a first-order model connected in series by L_1, L_2, L_3, and L_4. The transformer is an ideal transformer.

The photovoltaic LCL-T module has a higher order and is difficult to control. The introduction of the weighted current feedback method can use the zero-pole cancellation to make the mathematical model of the system first-order. Inversely infer its circuit model (see Figure 4), and analyze the Bode diagram to determine the feasibility of the model. The transformer adopts SZ11-20000/66kV, and any one-phase equivalent circuit of the LCL-T grid-connected inverter topology is set according to the following system parameters: L_1=0.033mH, L_2=0.007mH, C=500uF, L_3=L_4=2.63mH, L_m=5.94H. Keep L_3 and L_4 unchanged, reduce the L_1 parameter value by 40% and 60% respectively, observe the Bode diagram before and after the system is reduced, and the result is shown in Figure 5.

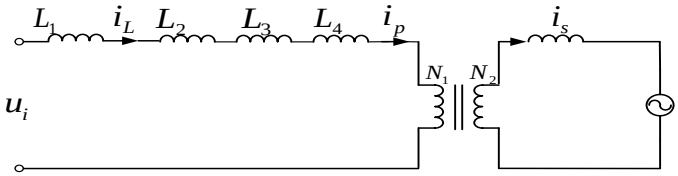

Figure 4: Equivalent Model of Reduced Order When Transformer is not Saturated

It can be seen from Figure 5 that the original system model has resonance spikes in the high frequency band, and the reduced system model is basically consistent with the original system model in the low frequency range, and the resonance spikes are eliminated in the high frequency band. Although the waveforms in the high frequency range are separated, which is not good consistent with the original system, the photovoltaic power generation system is integrated into the grid and adopts the power frequency, its ω value is within the range of the low frequency band, so the reduced-order equivalent model is feasible. At the same time, it is worth noting that the mathematical essence of the weighted current feedback method is to use the pole-zero cancellation to achieve the purpose of simplification. The transfer function converts the pole-zero point into an unobservable and real state quantity through a series of simplifications, which will continue to influence to the output of the system. Therefore, when the parameters of the LCL-T module change, it is necessary to discuss the influence of the parameter changes on the performance of the reduced-order equivalent model. This article takes the change of the filter inductance L1 as an example. From the comparison of the Bode diagrams before and after the reduction equivalent when the filter inductance L1 is reduced by 40% and 60% in Figure 5, it can be seen that the degree of coincidence with the original system of the low frequency band is not affected by the change of parameters. It has good robustness.

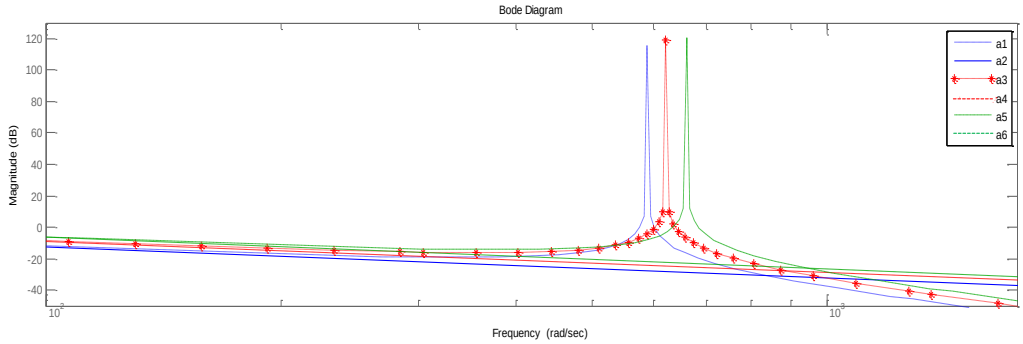

Figure 5: Bode Diagram Before and after Model Reduction

(a1 Original system model $G_{u_o \to i_{ps}}$; a2 reduced-order model $G_{u_o \to i_{ps}}$;a3 The original system model after 40% reduction $G_{u_o \to i_{ps}}$;a4 Reduced order model after 40% reduction $G_{u_o \to i_{ps}}$;a5 Original system model after 60% reduction $G_{u_o \to i_{ps}}$;a6 Reduced order model after 60% reduction $G_{u_o \to i_{ps}}$)

The reduced-order model based on the weighted current feedback method ignores the poor transient characteristics caused by the non-saturation of the transformer. In view of this shortcoming, the LCL-T reduced-order model based on the Routh approximation method is proposed below.

B. Order Reduction of LCL-T Module Based on Routh Approximation

The Routh approximation method is a method that uses advanced mathematical formulas to reduce the order of the high-order system. If the original system output is stable, then the reduced order equivalent system based on the Routh approximation method will also have good stability. The specific steps are as follows: first list the transfer function between the input and output of the system, then calculate the α, β parameters according to the transfer function, and get the Routh table based on the system stability judgment, and finally get the approximate transfer function of different orders according to the Routh table then complete the reduction equivalent processing of the system.

If the α-β parameter table is directly written according to the transfer function of the LCL-T module of the photovoltaic power generation system, the first-order expression of the transfer function is obtained. This approximation ignores the performance of the low frequency band. However, in the actual application of the photovoltaic power generation system, it usually adopt the power frequency, which belongs to the low frequency range. Therefore, the mathematical model of the LCL-T module (Equation 9) needs to be substituted in the form of $p=1/s$, and then:

$$\hat{G}_{u_i' \to i_{ps}'}(p) = 1/p\, G_{u_i' \to i_{ps}'}(1/p) = \frac{r_2 p^5 + a_5 p^4 + a_4 p^3 + a_3 p^2 + a_2 p + a_1}{r_m r_2 p^6 + b_6 p^5 + b_5 p^4 + b_4 p^3 + b_3 p^2 + b_2 p + b_1} \tag{17}$$

According to formula (17), the calculation of α and β parameters are shown in Table 1 and Table 2:

Table 1: α Parameter

	$r_m r_2$	b_5	b_3	b_1
	b_6	b_4	b_2	0
$\alpha_1 = r_m r_2 / b_6$	$\alpha_{11} = b_5 - \alpha_1 b_4$	$\alpha_{12} = b_3 - \alpha_1 b_2$	$\alpha_{13} = b_1$	$\alpha_{14} = 0$
$\alpha_2 = b_6 / \alpha_{11}$	$\alpha_{21} = b_4 - \alpha_2 \alpha_{12}$	$\alpha_{22} = b_2 - \alpha_2 \alpha_{13}$	$\alpha_{23} = 0$	$\alpha_{24} = 0$
$\alpha_3 = \alpha_{11} / \alpha_{21}$	$\alpha_{31} = \alpha_{12} - \alpha_3 \alpha_{22}$	$\alpha_{32} = b_1$	$\alpha_{33} = 0$	$\alpha_{34} = 0$
$\alpha_4 = \alpha_{21} / \alpha_{31}$	$\alpha_{41} = \alpha_{22} - \alpha_4 \alpha_{32}$	$\alpha_{42} = 0$	$\alpha_{43} = 0$	$\alpha_{44} = 0$
$\alpha_5 = \alpha_{31} / \alpha_{41}$	$\alpha_{51} = \alpha_{32}$	$\alpha_{52} = 0$	$\alpha_{53} = 0$	$\alpha_{54} = 0$

Table 2: β Parameter

	r_2	a_4	a_2	0
	a_5	a_3	a_1	0
$\beta_1 = r_2 / a_5$	$\beta_{11} = a_4 - \beta_1 a_3$	$\beta_{12} = a_2 - \beta_1 a_1$	$\beta_{13} = 0$	$\beta_{14} = 0$
$\beta_2 = a_5 / \beta_{11}$	$\beta_{21} = a_3 - \beta_1 \beta_{12}$	$\beta_{22} = a_1$	$\beta_{23} = 0$	$\beta_{24} = 0$
$\beta_3 = \beta_{11} / \beta_{21}$	$\beta_{31} = \beta_{12} - \beta_3 \beta_{22}$	$\beta_{32} = 0$	$\beta_{33} = 0$	$\beta_{34} = 0$
$\beta_4 = \beta_{21} / \beta_{31}$	$\beta_{41} = a_1$	$\beta_{42} = 0$	$\beta_{43} = 0$	$\beta_{44} = 0$

Taking the first-order approximation to the transfer function between the filter input voltage u_i' and the transformer primary output current i_{ps}', the first-order transfer function of the system can be obtained as shown in equation (18) by using the α_1 and β_1 parameters.

$$\hat{G}_{u_i' \to i_{ps}'}(p) = \beta_1 \frac{1}{1 + \alpha_1 p} \tag{18}$$

Restore and simplify formula (18) to:

$$G_{u_i' \to i_{ps}'}(s) = \frac{1}{\frac{r_m r_1 C + L_4 + 2r_2(r_1 + r_m)C}{r_2} + \frac{r_m r_2 [r_m r_1 C + L_4 + 2r_2(r_1 + r_m)C]}{r_2 N} s} \tag{19}$$

Where: $N = r_1 r_2 + r_m r_1^2 C + L_1 r_m + r_m(L_2 + L_3) + r_1 L_m + r_m^2 r_1 C + r_m r_2 + r_m L_4$

Since the reduced-order first-order transfer function cannot be directly reversed to the circuit model, the denominator is divided into two parts, namely the equivalent resistance Req and the equivalent inductance Leq, as shown in equations (20) and (21):

$$R_{eq} = \frac{r_m r_1 C + L_4 + 2r_2(r_1 + r_m)C}{r_2} \tag{20}$$

$$L_{eq} = \frac{r_m r_2[r_m r_1 C + L_4 + 2r_2(r_1 + r_m)C]}{r_2 N} \tag{21}$$

Substituting formula (20) and formula (21) into formula (19), the reduced-order equivalent model as shown in Figure 6 can be obtained by reversing, and the transformer is an ideal transformer.

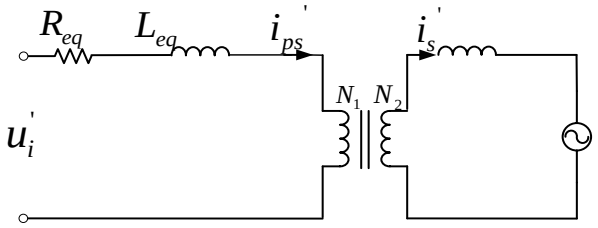

Figure 6: Reduced-order Equivalent Model When the Transformer is Saturated

The Bode diagram before and after the system is reduced is shown in Figure 6. It can be seen from Figure 6 that the system model after the order reduction eliminates the phenomenon of resonance spikes in the detailed model. When the ω value is in the range of 100~1000, the Bode diagrams before and after the order reduction are more consistent, and the photovoltaic power generation system is integrated into the power grid using power frequency. The ω value is within the coincidence range, so the reduced-order model is feasible. When the parameters of the LCL-T module change, take changing the filter inductance L1 as an example. According to the comparison of the Bode diagram before and after the reduction equivalent when the filter inductance L1 is reduced by 40% and 60% (see Figure 7), The coincidence of the power frequency band is not affected by the change of the parameters, and has good robustness.

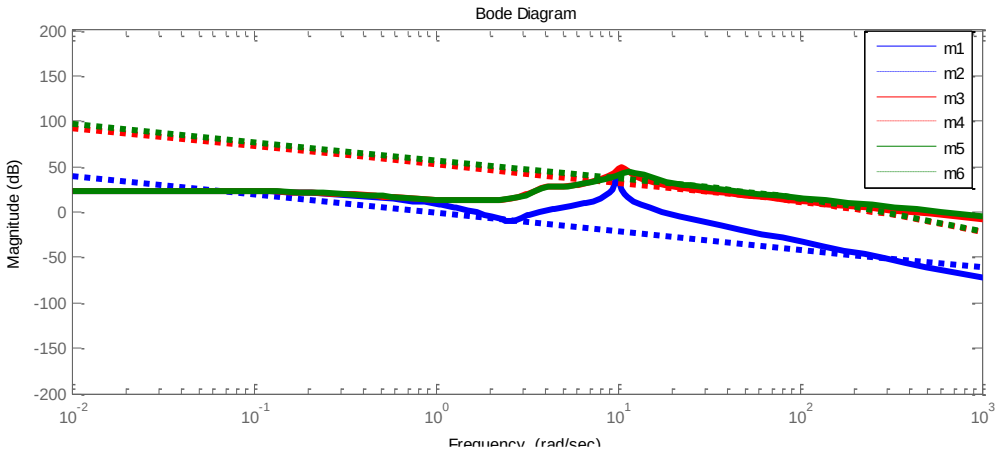

Figure 7: Bode Diagram Before and after Model Reduction

(m1:Original system model $G_{u_o \to i_{ps}}$; m2:Reduced model $G_{u_o \to i_{ps}}$; m3 The original system model after 40% reduction $G_{u_o \to i_{ps}}$; m4 Reduced order model after 40% reduction $G_{u_o \to i_{ps}}$; m5 Original system model after 60% reduction $G_{u_o \to i_{ps}}$; m6 Reduced order model after 60% reduction $G_{u_o \to i_{ps}}$;)

IV. Simulation Results and Analysis

Take the 20MW photovoltaic power generation system as an example, the transformer model adopts SZ11-20000/66kV. Photovoltaic array parameters: the number of photovoltaic array modules in series N_1=325, the number of parallel modules N_2=100, the number of batteries connected in series per module n_1=32, the number of batteries connected in parallel per module n_2=6, the reference illumination intensity is 1000W/m^2, the reference

temperature is 25℃, set the illumination intensity to 400W/m2, and the working temperature is the reference temperature; The LCL filter parameters: L_1=0.0042H, L_2=0.0099H, C=1.5uF; Transformer parameters: L_3=L_4=0.0173mH, r_1=r_2=0.023Ω.

A. *Formula for Calculating Deviation*

Variables for deviation calculation include active power, reactive power, line voltage and phase current of the grid connection point. X_{det} and X_{eq} are used to represent the unit value of the detailed model and equivalent model data of the above electrical parameters. The sequence numbers of the first and last data of the detailed model and the equivalent model of the corresponding interval are represented by K_{det_s}, K_{eq_s} and K_{det_e}, K_{eq_e}, respectively.

The deviation calculation method is as follows:

1) The average deviation F1 of the steady-state interval is:

$$F_1 = \left| \frac{1}{K_{eq\_e} - K_{eq\_s} + 1} \sum_{i=K_{eq\_s}}^{K_{eq\_e}} X_{eq}(i) - \frac{1}{K_{\det\_e} - K_{\det\_s} + 1} \sum_{i=K_{\det\_s}}^{K_{\det\_e}} X_{\det}(i) \right| \tag{22}$$

2) The average deviation F2 of the transient interval is:

$$F_2 = \left| \frac{1}{K_{eq\_e} - K_{eq\_s} + 1} \sum_{i=K_{eq\_s}}^{K_{eq\_e}} X_{eq}(i) - \frac{1}{K_{\det\_e} - K_{\det\_s} + 1} \sum_{i=K_{\det\_s}}^{K_{\det\_e}} X_{\det}(i) \right| \tag{23}$$

3) The maximum deviation F3 of the steady-state interval is:

$$F_3 = \max_{i=K_{\det\_s}..K_{\det\_e}} \left(\left| X_{\det}(i) - X_{eq}(i) \right| \right) \tag{24}$$

B. *Photovoltaic Grid-connected Steady-state Conditions*

The influence of temperature change of photovoltaic power generation system during the day on the output characteristics is relatively small compared with the illumination intensity, so this article only compares and analyzes different light intensities, set the external temperature as the reference temperature, and the simulation duration is 0.5s.

Figure 8 shows the comparison results of the active power, reactive power and line of the photovoltaic power generation system based on the detailed model of the LCL-T module (blue) and the reduced-order model (red) proposed in this article under steady-state conditions and 400W/m2 of illumination intensity.

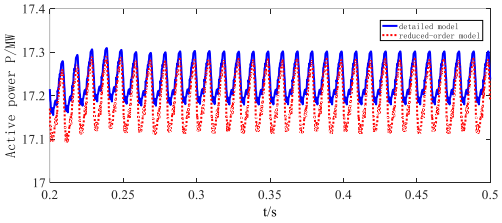

a) Active power at grid connection point

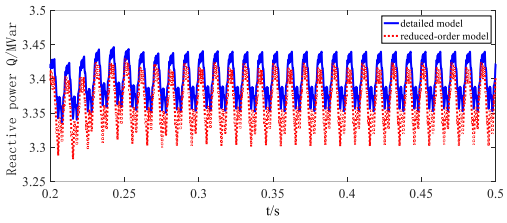

b) Reactive power at grid connection point

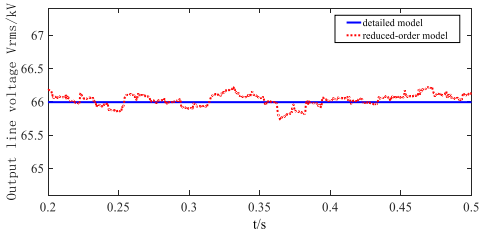

c) Line voltage of grid-connected point

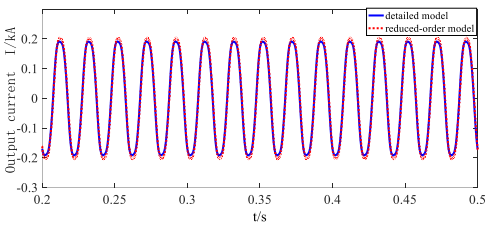

d) Output current of grid-connected point

Figure 8: Comparison of Output Waveforms of Photovoltaic Grid Points Based on the Detailed Model of the Lcl-T Module and the Reduced-order Model Proposed in This Article

The maximum allowable deviation of active power, reactive power, line voltage and phase current of the reduced-order model of photovoltaic power generation system under steady-state conditions should not exceed 15%, 15%, 5%, and 15% [5], respectively. It can be seen from Figure 8 that due to neglect of switching losses when equivalent to power electronic devices, both active power and reactive power are reduced, and the phase current is slightly increased. However, from a general point of view, the maximum deviation of active power at the grid-connected point is 0.42%, the maximum deviation of reactive power is 1.76%, the maximum deviation of

output line voltage is 0.4%, the maximum deviation of output phase current is 2.42%, and the deviation of each variable is within the allowable range. The reduced-order model proposed in this article and the detailed model has a high degree of agreement.

Table 3 shows the maximum deviation of each variable when the illumination intensity is 600W/m2, 800W/m2, 1000W/m2. From Table 3, we can see that the maximum deviation of each variable does not exceed 3%. The reduced-order model proposed in this article and the detailed model has a high degree of agreement and good robustness.

Table 3: Maximum Deviation of Each Variable under Different Constant Illumination Intensity

Illumination intensity (W/m2)	Maximum deviation (%)			
	Active power	Reactive power	Output line voltage	Output current
600	0.60	2.65	0.61	2.40
800	0.83	2.36	0.48	2.64
1000	0.74	2.01	0.62	2.47

C. Transient Conditions of Photovoltaic Grid-connected

Taking illumination intensity disturbance and three-phase short circuit faults as examples, the dynamic response capability of the reduced-order model proposed in this paper is analyzed.

Case 1: The simulation time is 2s, the actual temperature is the reference temperature, the initial light intensity of the photovoltaic power generation system is 800W/m2, drops to 400W/m2 at 0.5s, and increases to 1000W/m2 at 1s, and then remains unchanged.

Figure 9 shows the conditions under the illumination intensity disturbance, the comparison results of the simulation waveforms of the active power, reactive power, line voltage and phase current at the grid connection of the photovoltaic power generation system based on the detailed model of the LCL-T module (blue) and the reduced-order model (red) proposed in this paper.

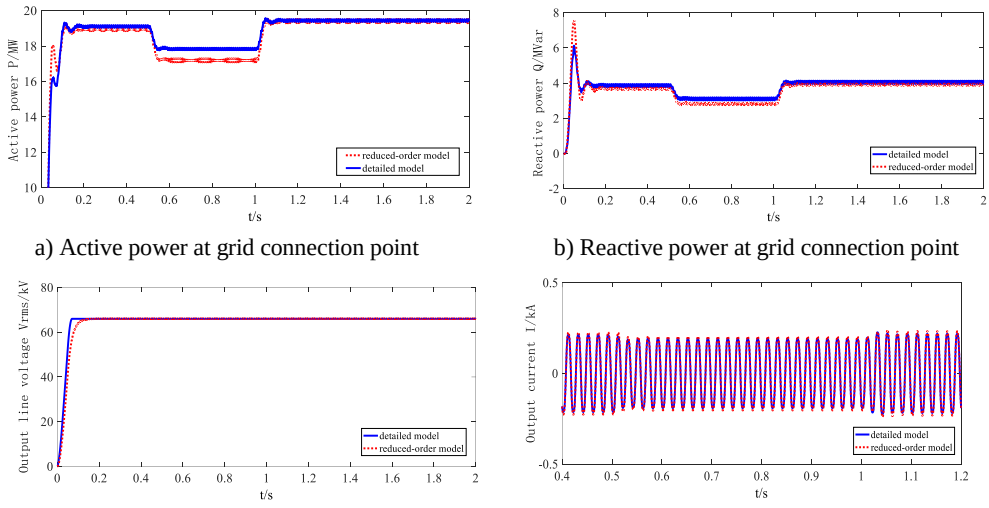

a) Active power at grid connection point

b) Reactive power at grid connection point

c) Line voltage of grid-connected point

d) Output current of grid-connected point

Figure 9: Comparison of Output Waveforms of Photovoltaic Grid-Connected Points Based on the Detailed Lcl-T Module and the Reduced-order Model Proposed in this Article

Under transient conditions, the average deviation of active power, reactive power, line voltage and phase current of the reduced-order model of photovoltaic power generation system is 20%, 20%, 5%, 20% in the transient interval [5], and in the steady-state interval are 10%, 10%, 2% and 10%.

As shown in Figure 9, the illumination intensity disturbance operating condition is similar to the grid-connected steady-state operating condition of the photovoltaic power generation system. Since the switching loss is ignored when the power electronic devices are equivalent, the active power and reactive power are reduced; the waveform of the phase current fluctuates slightly because there is no grid-side clamp; and the waveform of the line voltage is relatively stable under the dual effects of grid voltage clamping and photovoltaic power generation system control strategy.

From the average deviation of each variable shown in Table 4, it can be seen that the maximum deviation of the transient interval is 9.36% under the condition of light intensity disturbance, which is slightly larger than the

average deviation of the steady-state interval, but the average deviation of each variable is within the allowable value range. The reduced-order model proposed in this article and detailed model has a high degree of agreement.

Table 4: The Average Deviation of Each Variable under the Light Intensity Disturbance Condition

variable	Average deviation (%)	
	Steady state interval	Transient interval
Active power	0.78	3.49
Reactive power	4.88	9.36
Line voltage	0.01	0.01
Phase current	6.46	6.53

Case 2: The simulation time is 2s, the actual temperature is the reference temperature, the light intensity is 800W/m2, and the grid-connected distance is 5.8km. When t=1s, a three-phase short-circuit fault occurs at the output point of the photovoltaic power station 1km, and the grounding resistance is 0.2Ω. Remove the fault at t=1.1s.

Figure 10 shows the simulation waveform comparison result of active power, reactive power, line voltage, and phase current of photovoltaic power generation system grid-connected points based on the detailed model of the LCL-T module (blue) and the reduced-order model (red) proposed in this article under three-phase short-circuit conditions. As shown in Figure 10, under three-phase short-circuit conditions, although the active power, reactive power and line voltage have slight oscillations during the transient process, they still have good dynamic response characteristics. The average deviation of the variables shown in Table 5 shows that the average deviation of each variable is within the allowable range.

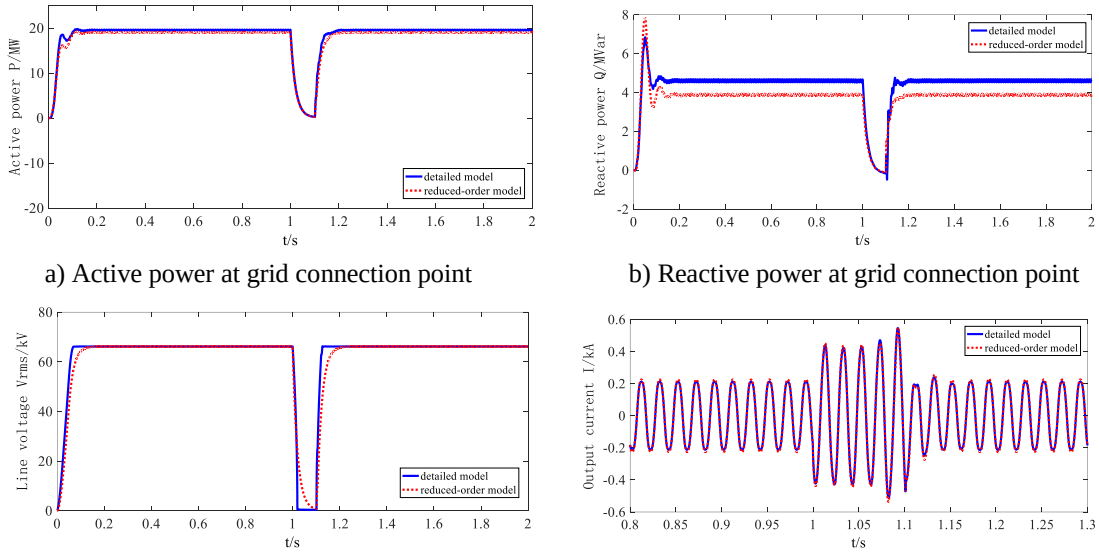

a) Active power at grid connection point

b) Reactive power at grid connection point

c) Line voltage of grid-connected point

d) Output current of grid-connected point

Figure 10: Comparison of Output Waveforms of Photovoltaic Grid Points Based on the Detailed Lcl-T Module and the Reduced-order Model Proposed in this Article

Table 5: Average Deviation of Each Variable under Three-Phase Short Circuit Conditions

variable	Average deviation (%)	
	Steady state interval	Transient interval
Active power	2.76	3.46
Reactive power	4.31	5.77
Line voltage	0.45	4.20
Phase current	7.17	7.31

D. The speed-up test of the reduced-order model proposed in this paper

Build 5 photovoltaic power generation systems with a capacity of 20MW, and connect them to the 66kV grid. The simulation time is 2s, the temperature is 25℃, and the light intensity is 400W/m2, 600W/m2, 800W/m2, 1000W/m2, respectively. Taking the average of 10 sets of actual running time, the comparison of the simulation time of the comparison of photovoltaic grid-connected system based on the detailed LCL-T module and the reduced-order model proposed in this paper is shown in Table 3.

Table 6: Comparison of Simulation Time of Photovoltaic Grid-connected System Based on the Detailed Lcl-T Module and the Reduced-order Model Proposed in This Paper

light intensity (W/m^2) /temperature 25℃	Detailed model simulation time (s)	Reduced model simulation time (s)
400	874	13
600	895	17
800	901	21
1000	896	23

It can be seen from Table 6 that the simulation time of the reduced-order model proposed in this paper is significantly shortened, and the speed-up effect is significant compared with the detailed model.

V. CONCLUSIONS

This paper presents a LCL-T reduced-order model of the AC side of the photovoltaic power generation system to adapt to the large-scale grid connection of offshore wind power. Considering the saturation and non-saturation of the transformer, when the transformer is not saturated, the LCL-T reduced-order model based on the weighted current feedback method is used to achieve the purpose of simplification through the zero-pole cancellation of the transfer function; when the transformer is saturated, the LCL-T module reduction method based on the Routh approximation method is used, and the higher-order system is reduced by the advanced mathematical formula, the following results can be obtained through PSCAD/EMTDC simulation.

The output active power, reactive power, and excitation inrush current waveforms of the reduced-order model in both cases of transformer saturation and non-saturation can be in good agreement with the detailed model and has good dynamic and static response capabilities to meet the external characteristics of the photovoltaic power generation system; The reduced-order model can effectively shorten the simulation time and has high accuracy.

The reduced-order model has a simple structure and can provide new ideas for the design of the intermediate links of the photovoltaic power generation system (that is, the inverter and its control). However, due to the oversimplification of the model, the new simulation model cannot effectively simulate the internal characteristics of photovoltaic array systems. Therefore, the equivalent model proposed in this paper cannot be used for the study of the internal characteristics of photovoltaic array systems. Subsequent research can start from this and explore efficient reduced order models applicable to the internal characteristics of photovoltaic systems.

REFERENCES

[1] Trapani K, Millar D L, Smith H C. Novel offshore application of photovoltaics in comparison to conventional marine renewable energy technologies. Renewable Energy, 2013, 50(FEB.):879-888.

[2] Trapani K , Millar D L. Proposing offshore photovoltaic (PV) technology to the energy mix of the Maltese islands.Energy Conversion & Management, 2013, 67(01):18-26.

[3] Hasan A, Dincer I. A new performance assessment methodology of bifacial photovoltaic solar panels for offshore applications. Energy Conversion and Management, 2020, 220:112972.

[4] Mannan J, Kamran M A, Ali M U, Mannan MMN. Quintessential strategy to operate photovoltaic system coupled with dual battery storage and grid connection. International Journal of En-ergy Research. 2021, 45(15):21140-21157.

[5] Arias Garcia, Rodolfo Manuel, Perez Abril, Ignacio. Photovoltaic module model determination by using the Tellegen's theorem. Renewable Energy, 2020, 152(01):409-420.

[6] Manish P, Yak S K. Extraction of Equivalent Noise Source Model From Photovoltaic Systems. IEEE Transactions on Electromagnetic Compatibility, 2019, 61(03):903-910.

[7] Madi S, Kheldoun A. Bond graph based modeling for parameter identification of photovoltaic module. Energy, 141(01): 1456-1465.

[8] Chaibi Y, Allouhi A, Malvoni M, Salhi M, Saadani R. Solar irradiance and temperature influence on the photovoltaic cell equivalent-circuit models. Solar Energy, 2019, 188(01):1102-1110.

[9] Shamsodin T, Khenar M, Hosseini S K, Cretu AM, Taheri H. PSO-based Model and analysis of Photovoltaic Module Characteristics in Snowy Conditions. IET Renewable Power Generation, 2019, 13(11):1950-1957.

[10] Prakash SB, Singh G, Singh S. Modeling and Performance Analysis of Simplified Two-Diode Model of Photovoltaic Cells. Frontiers in Physics, 2021-11-18.

[11] L Wang, P Sun, J Wang, K Zhu, Y Zhang. A Delay Compensation Method to Improve the Current Control Performance of the LCL-Type Grid-Connected Inverter//2019 IEEE 10th International Symposium on Power Electronics for Distributed Generation Systems (PEDG). IEEE, 2019.

[12] G Shen, X Zhu, J Zhang, D Xu. A new feedback method for PR current control of LCL- filter-based grid-connected inverter. IEEE Transac- tion on Industry Electronics, 2010, 57(6): 2033-2041.

[13] G. Shen, D. Xu. Current Control for Grid-connected Inverters by Splitting the Capacitor of LCL Filter. Proceedings of the CSEE, 2008(18):36-41.

[14] C. Hei, Y. Guan, Y, Xie. Simulation analysis of distribution network with distributed photovoltaic generation system based on Thevenin-Norton equivalence. Electric power automation equipment.2017, 37(10):71-78.

[15] Rick Wallace Kenyon, Amirhossein Sajadi, Andy Hoke, Bri-Mathias Hodge. Open-Source PSCAD Grid-Following and Grid-Forming Inverters and A Benchmark for Zero-Inertia Power System Simulations//2021 IEEE Kansas Power and Energy Conference (KPEC).IEEE, 2021.

[16] H Yuan, Reetam Sen Biswas, J Tan, Y Zhang. Developing a Reduced 240-Bus WECC Dynamic Model for Frequency Response Study of High Renewable Integration//2020 IEEE/PES Transmission and Distribution Conference and Exposition (T&D). IEEE, 2020.

[17] Pitambar Jankee, Hilary Chisepo, Victor Adebayo, David Oyedokun, Charles Trevor Gaunt. Transformer models and meters in MATLAB and PSCAD for GIC and leakage dc studies//2020 International SAUPEC/RobMech/PRASA Conference, Cape Town, South Africa, 2020.

[18] MemonAP, UqailiMA, MemonZA. Time Frequency Analysis Techniques for Detection of Power System Transient Disturbances. International Journal of Emerging Trends in Electrical and Electronics, 2013, 9(1): 2320-9569.

[19] L Hong L, X Zhou, H Xia, Y Liu, A Luo. Mechanism and Prevention of Commutation Failure in LCC-HVDC Caused by Sending End AC Faults. IEEE Transactions on Power Delivery, 2021, 36(1):473-476.

[20] JS Huh, WS Moon, BW Kang, JC Kim, HS Shin. Analysis of transformer inrush current of electric railways with automatic power changeover switch system. ICIC Express Letters, 2014, 8(5):1237-1242.